Available online at www.sciencedirect.com

SCIENCE DIRECT

Virology 333 (2005) 54–65

VIROLOGY

www.elsevier.com/locate/yviro

Ca^{2+} permeability of the plasma membrane induced by rotavirus infection in cultured cells is inhibited by tunicamycin and brefeldin A

Marie Christine Ruiz*, Yuleima Díaz, Franshelle Peña, Olga C. Aristimuño, Maria Elena Chemello, Fabian Michelangeli

Laboratorio de Fisiología Gastrointestinal, Instituto Venezolano de Investigaciones Científicas, Caracas 1020A, Venezuela

Received 29 September 2004; returned to author for revision 18 November 2004; accepted 5 December 2004
Available online 28 January 2005

Abstract

Rotavirus infection of cultured cells induces a progressive increase in plasma membrane permeability to Ca^{2+}. The viral product responsible for this effect is not known. We have used tunicamycin and brefeldin A to prevent glycosylation and membrane traffic and study the involvement of viral glycoproteins, NSP4 and/or VP7, in rotavirus-infected HT29 and MA104 cells. In infected cells, we observed an increase of plasma membrane Ca^{2+} permeability and a progressive depletion of agonist-releasable ER pools measured with fura 2 and an enhancement of total Ca^{2+} content measured as $^{45}Ca^{2+}$ uptake. Tunicamycin inhibited the increase in membrane Ca^{2+} permeability, induced a depletion of agonist-releasable and $^{45}Ca^{2+}$-sequestered pools. Brefeldin A inhibited the increase of Ca^{2+} permeability and the increase in $^{45}Ca^{2+}$ uptake induced by infection. We propose that the glycosylated viral product NSP4 (and/or VP7) travels to the plasma membrane to form a Ca^{2+} channel and hence elevate Ca^{2+} permeability.

Keywords: Ionic viral pathway; Calcium pools; Calcium permeability; Calcium homeostasis; Rotavirus; HT29 cells; MA104 cells

Introduction

Many animal viruses produce a lytic infection of the host cell. Cell lysis is usually the consequence of disturbances in cell function as a result of viral genome expression and viral protein synthesis. The main alteration is a progressive change in membrane permeability to both monovalent and divalent cations and then to macromolecules of increasing size. These last ones are provoked by a disruption of membrane integrity preceding cell death. Two aspects are fundamental in understanding the mechanisms of cell permeabilization and lysis by viral infections: (a) the nature of the cell membrane modifications at the molecular level; and (b) the identity of the viral products responsible for these modifications (Carrasco, 1995).

Rotaviruses are non-enveloped viruses belonging to the Reoviridae family. Their segmented dsRNA genome is contained within an icosahedral capsid organized in three concentric layers. The most internal layer is formed by VP2 and encloses the genome that codes for six structural and five non-structural proteins. The viral protein VP6 is the only component of the intermediate layer. The outer shell consists of the glycoprotein VP7 and VP4 that is organized in dimers to form 60 spikes.

The viral cycle has been mainly studied in cultured MA104 cells. Rotavirus uses the endoplasmic reticulum (ER) for its assembly and maturation (Estes, 1996). Double layer particles (DLP) are assembled in the cytoplasm and bud into the ER through the interaction between VP6 and the non-structural viral protein NSP4, which plays the role of a viral receptor in the ER membrane. NSP4 is a glycosylated integral ER membrane protein. During the budding process, viral particles transiently acquire ER membrane containing VP7. Once inside the ER lumen, there is a selective segregation of membrane lipids and NSP4, and the outer

* Corresponding author. Fax: +58 212 504 1093.
E-mail address: mclr@ivic.ve (M.C. Ruiz).

0042-6822/$ - see front matter © 2005 Elsevier Inc. All rights reserved.
doi:10.1016/j.virol.2004.12.032

layer containing VP7 and VP4 is assembled. The acquisition of VP4, a cytoplasmic synthesized protein, is not yet clear (Delmas et al., 2004). Mature virus is thought to be retained in the ER and then released by cell lysis (Michelangeli et al., 1991). However, in differentiated and polarized Caco2 cells rotavirus particles seem to be released at the apical pole of the cell without lysis (Jourdan et al., 1997).

Rotavirus infection of cultured cells induces changes in the homeostasis of calcium that appear to be mediated by the synthesis of viral proteins (del Castillo et al., 1991; Michelangeli et al., 1991, 1995). Among these perturbations we have measured a progressive increase in Ca^{2+} plasma membrane permeability, which leads to an elevation of cytosolic Ca^{2+} concentration and an enhancement of sequestered Ca^{2+} pools sensitive to thapsigargin, an inhibitor of ER Ca^{2+} ATPase (Michelangeli et al., 1991, 1995). This effect is likely due to the activation of ER Ca^{2+} pumps.

The viral product responsible for the change of Ca^{2+} permeability is not known. However, NSP4 appears as a likely candidate given its many effects on Ca^{2+} homeostasis (Estes, 2003; Estes et al., 2001; Michelangeli and Ruiz, 2003; Ruiz et al., 2000). Expression of recombinant NSP4 in insect cells (Sf9) induced a change in Ca^{2+} concentration, although without changes in Ca^{2+} permeability of the plasma membrane (Tian et al., 1994). Furthermore, inducible intracellular expression of NSP4-EGFP fusion protein in mammalian HEK 293 cells elevates basal intracellular calcium levels more than twofold by a phospholipase C independent mechanism (Berkova et al., 2003). In various virus groups, different proteins are able to induce ionic pathways modifying cell membrane permeability (Gonzalez and Carrasco, 2003). These can be structural or non-structural proteins, which play a role in the entry mechanism or later during viral replication and pathogenesis.

In this work, we have studied the possible involvement of NSP4 (and/or VP7) in the alteration of Ca^{2+} plasma membrane permeability induced by rotavirus. We have used tunicamycin (TM), an N-glycosylation inhibitor, and brefeldin A (BFA), a compound that blocks protein export from the endoplasmic reticulum (ER) to the Golgi complex to prevent normal glycosylation and membrane traffic (Lippincott-Schwartz et al., 1991; Orci et al., 1991).

Results

Infection induces an increase of plasma membrane Ca^{2+} permeability and a perturbation of Ca^{2+} pools

We have studied the relationship between infection, Ca^{2+} permeability, and agonist-releasable Ca^{2+} pools in HT29 and MA104 cells loaded with fura 2. In infected cells, the addition of Ca^{2+} (5 mM) to the extracellular medium induced an increase in cytoplasmic Ca^{2+} concentration ($[Ca^{2+}]_i$), whereas almost no change was observed in non-infected cells (Fig. 1, upper traces). Although the increase in $[Ca^{2+}]_i$ is

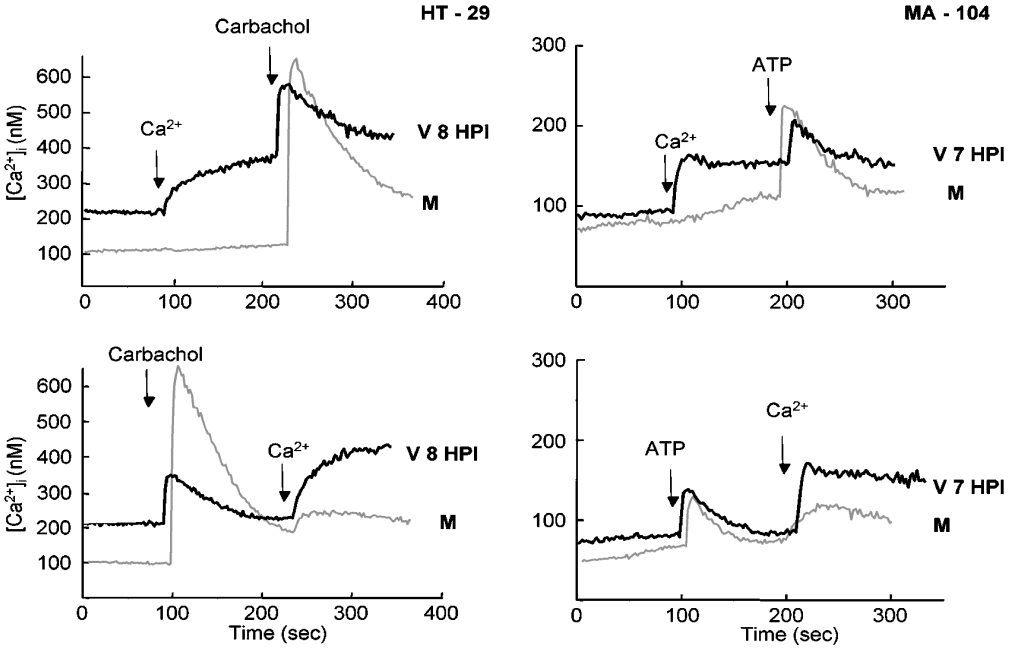

Fig. 1. Increase in plasma membrane permeability to Ca^{2+} and decrease in agonist-releasable Ca^{2+} pools in rotavirus-infected HT29 and MA104 cells. Confluent monolayers of HT29 and MA104 cells grown in 75 cm^2 falcon flasks were infected with the OSU strain of rotavirus (see Materials and methods). Mock-infected cells were kept as controls. At given times post-infection, HT29 (8 HPI) and MA104 (7 HPI) monolayers were trypsinized, and cell suspensions were loaded with fura 2 for the measurement of $[Ca^{2+}]_i$. Permeability to Ca^{2+} in rotavirus (V)- or mock (M)-infected cells was evaluated by the change in $[Ca^{2+}]_i$ induced by the addition of 5 mM $CaCl_2$ to the extracellular medium, which initially contained 1 mM Ca^{2+}. The state of filling of agonist sensitive sequestered Ca^{2+} pools was evaluated using carbachol (10 μM) in HT29 cells or ATP (250 μM) in MA104 cells. Results of a representative experiment of a series are shown (HT29 upper traces, $n = 11$; HT29 lower traces, $n = 13$; MA104 upper traces, $n = 21$; MA104 lower traces, $n = 9$).

the result of a balance between calcium entry and regulatory processes, the change in $[Ca^{2+}]_i$ during the first few seconds reflects the state of plasma membrane permeability (Perez et al., 1999). Actinomycin D added at one post-infection had no effect on the increase of Ca^{2+} permeability induced by rotavirus infection in MA104 cells (results not shown). Therefore, we may conclude that during rotavirus infection there is an increase of Ca^{2+} permeability related to the synthesis of a viral product and not to the de novo synthesis of a cellular protein.

To evaluate the state of filling of agonist sensitive sequestered Ca^{2+} pools we used carbachol or ATP in HT29 and MA104 cells, respectively. These cells express specific muscarinic and purinergic receptors to these agonists. As observed in Fig. 1 (upper traces), carbachol or ATP added to infected or non-infected cells after the 5-mM Ca^{2+} pulse caused a fast rise in $[Ca^{2+}]_i$ corresponding mostly to the release of stored Ca^{2+}. The amount of Ca^{2+} released by the agonists in infected cells was considerably lower than in controls. However, the peak $[Ca^{2+}]_i$ attained was rather similar in non-infected and infected cells and for both cell types due to the fact that the starting level was much higher in the infected cells. This decrease of store size in infected cells could be better observed when carbachol was added first as seen in the lower traces (Fig. 1). The peak $[Ca^{2+}]_i$ in infected cells was much lower than in non-infected ones. This effect was more evident in HT29 than MA104 cells. As observed in the same traces, after agonist stimulation the addition of 5 mM Ca^{2+} to the extracellular medium provoked a new increase in Ca^{2+} concentration in infected as well as in non-infected cells. In the case of non-infected cells, we could at this point measure a sizable Ca^{2+} permeability. This increase of permeability in control cells could be linked to store depletion induced by the agonist that activates a capacitative channel and Ca^{2+} entry (Carafoli, 2002). In the case of infected cells, Ca^{2+} entry after agonists was higher than in mock-infected cells, suggesting the participation at least two pathways: the capacitative and virus-induced channels in parallel.

Tunicamycin inhibits the increase of plasma membrane Ca^{2+} permeability induced by rotavirus infection

Perturbation of Ca^{2+} homeostasis during rotavirus infection has been linked to the synthesis of a viral product (Michelangeli et al., 1991). On the other hand, expression of the glycoprotein NSP4 has been associated to the increase in $[Ca^{2+}]_i$ (Tian et al., 1994). Therefore, we have used tunicamycin to prevent glycosylation of viral proteins and assess the putative involvement of NSP4 (and/or VP7) in this effect. We measured cytosolic Ca^{2+} concentration, plasma membrane Ca^{2+} permeability, and the state of Ca^{2+} pools in HT29 and MA 104 cells.

Tunicamycin had no effect on the plasma membrane Ca^{2+} permeability or the state of the Ca^{2+} pools of mock-infected HT29 and MA104 cells (Fig. 2, upper traces). However, this drug had a striking effect on rotavirus-infected cells. Treatment of infected cells with tunicamycin reduced the rise in $[Ca^{2+}]_i$ upon addition of 5 mM Ca^{2+} to the extracellular medium (Fig. 2, upper traces).

The results of a series of experiments in both cell types are analyzed in Fig. 3. We have to point out that the experiments in MA104 cells were performed at 5 h post-infection since tunicamycin reduces cell viability in infected cells at longer times. Plasma membrane permeability is evaluated measuring the concentration of Ca^{2+} attained after the addition of 5 mM Ca^{2+} (Figs. 3A and B) and calculating the initial rate of change of $[Ca^{2+}]_i$ (dCa^{2+}/dt; Figs. 3C and D). Although almost no change in basal $[Ca^{2+}]_i$ could be detected in virus-infected cells at these early times post-infection, we already observed a significant increase in the initial rate and the maximal $[Ca^{2+}]_i$ attained after the Ca^{2+} pulse elicited by virus infection in HT29 and MA104 cells. Tunicamycin significantly reduced the increase in $[Ca^{2+}]_i$ attained after the Ca^{2+} pulse and the initial rate in rotavirus-infected cells, corresponding to a partial inhibition of virus-induced Ca^{2+} permeability in both cell lines.

To evaluate the effect of tunicamycin on the state of filling of agonist sensitive sequestered Ca^{2+} pools we induced the release of stored Ca^{2+} with carbachol or ATP (Fig. 2). When the agonists were added after the 5-mM Ca^{2+} pulse (Fig. 2, upper traces), the $[Ca^{2+}]_i$ attained in rotavirus-infected cells treated with tunicamycin was much smaller than that elicited in untreated infected cells. When carbachol or ATP were added in normal extracellular Ca^{2+} concentration, the effect of tunicamycin was even more evident (Fig. 2, lower traces and Figs. 3E and F). Therefore, in rotavirus-infected cells tunicamycin induced a further depletion of Ca^{2+} pools sensitive to agonists, whereas no effect was observed in mock-infected cell.

The addition of 5 mM Ca^{2+} after stimulation with carbachol or ATP leads to an increase in Ca^{2+} concentration in mock- and rotavirus-infected cells treated or not with tunicamycin. However, as in the case of Fig. 1, the increase in Ca^{2+} concentration in mock-infected cells was small and probably attributable to capacitative Ca^{2+} entry. In the case of virus-infected cells $[Ca^{2+}]_i$ increase was much larger than that observed in mock-infected cells, which we have associated above to the activation of a virus-induced pathway and capacitative Ca^{2+} entry. In rotavirus-infected cells tunicamycin treatment reduced Ca^{2+} entry after agonists with respect to untreated ones (Fig. 2, lower traces). This confirms the inhibition by tunicamycin of virus-induced Ca^{2+} permeability.

In previous reports we showed that Ca^{2+} pools measured as $^{45}Ca^{2+}$ uptake progressively increased during the viral cycle (Michelangeli et al., 1991, 1995). This increase was sensitive to thapsigargin an inhibitor of the SERCA pump, indicating that Ca^{2+} was accumulated in the ER during infection. To evaluate the effect of tunicamycin on total Ca^{2+} pools during the viral cycle, we measured $^{45}Ca^{2+}$ uptake in

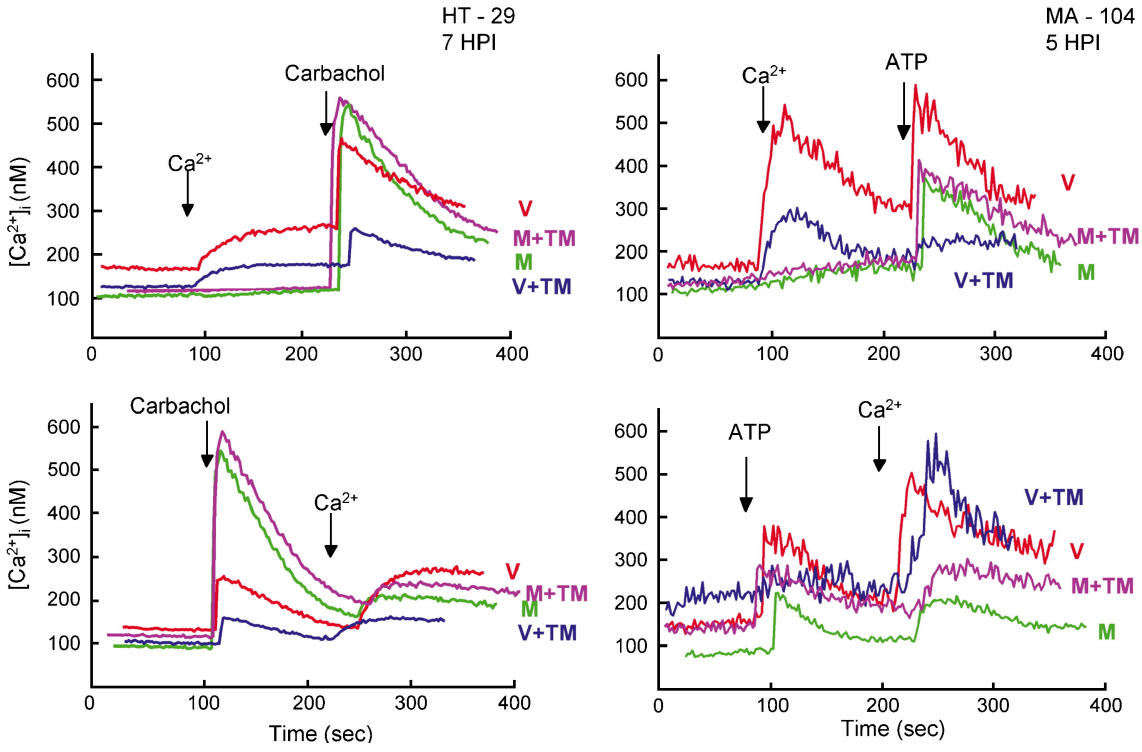

Fig. 2. Effect of tunicamycin on plasma membrane permeability to Ca^{2+} and on agonist-releasable Ca^{2+} pools in rotavirus- or mock-infected HT29 and MA104 cells. Confluent monolayers of HT29 and MA104 cells grown in 75 cm^2 falcon flasks were infected (V) as described (see Materials and methods). Mock-infected cells (M) were kept as controls. At 1 h post-infection the inoculum was removed and the replaced by a medium with or without tunicamycin (TM; 5 μg/ml). At given times post-infection, HT29 (7 HPI) and MA104 (5 HPI) monolayers were trypsinized and cell suspensions were loaded with fura 2 for the measurement of $[Ca^{2+}]_i$. Permeability to Ca^{2+} and the state of filling of agonist sensitive sequestered Ca^{2+} pools were evaluated as described in Fig. 1. Traces of a representative experiment for each cell type are shown (HT29 upper traces, $n = 6$; HT29 lower traces, $n = 5$; MA104 upper traces, $n = 11$; MA104 lower traces, $n = 4$).

MA104 cells. As earlier shown, rotavirus infection induced an increase of $^{45}Ca^{2+}$ uptake (Fig. 4). The presence of tunicamycin blocked this increase of $^{45}Ca^{2+}$ uptake.

The tunicamycin effect was dependent on the time of addition of the agent (Fig. 5). When tunicamycin was added at 1 h post-infection and $^{45}Ca^{2+}$ uptake was measured at 8 h post-infection, there was a complete reduction of the amount of $^{45}Ca^{2+}$ taken up by the cell as already observed in Fig. 4. When tunicamycin was added later in the viral cycle the effect faded out observing a small inhibition if the agent was added at four post-infection and no effect at 6 h. It should be pointed out that tunicamycin had no effect whatsoever on $^{45}Ca^{2+}$ uptake in mock-infected cells up to 8 h of incubation. These results indicate that in infected cells under tunicamycin treatment the ER is unable to accumulate Ca^{2+} above the mock-infected cell values.

The results suggest that the synthesis of a glycosylated viral product accumulated during the first 4–6 h post-infection is related to the increase in Ca^{2+} permeability and $^{45}Ca^{2+}$ uptake. Since tunicamycin reduces Ca^{2+} permeability induced by infection, the amount of Ca^{2+} that can be taken up from the cytoplasm into the ER may be decreased. This interpretation is further supported by earlier results obtained in our laboratory in which cycloheximide, but not actinomycin D, inhibited virus infection-induced $^{45}Ca^{2+}$ uptake when it was added at 1 HPI but not later after 5 HPI (Michelangeli et al., 1991).

The evaluation of Ca^{2+} pools releasable by agonists as measured by fura 2, or by $^{45}Ca^{2+}$ uptake, suggests an apparent contradiction. In the first case the amount of Ca^{2+} released by agonists tends to decrease (specially in HT29) whereas there is a striking accumulation of $^{45}Ca^{2+}$ in the infected MA104 cell. The difference may be in the fact that the first method measures free Ca^{2+} whereas the other estimates total Ca^{2+} content sensitive to thapsigargin.

Brefeldin A inhibits the increase of Ca^{2+} permeability in rotavirus-infected cells

To evaluate the possibility of a protein traveling to the plasma membrane via the secretory pathway to increase Ca^{2+} permeability, we studied the effects of brefeldin A, an inhibitor of protein traffic between the ER and the Golgi complex (Lippincott-Schwartz et al., 1991). We measured Ca^{2+} permeability and agonist-releasable Ca^{2+} pools in fura 2 loaded HT29 and MA104 cells. Brefeldin A added from 1 h post-infection induced a partial inhibition of Ca^{2+} permeability in rotavirus-infected cells as evaluated by the addition of a 5-mM extracellular Ca^{2+} pulse (Fig. 6, upper

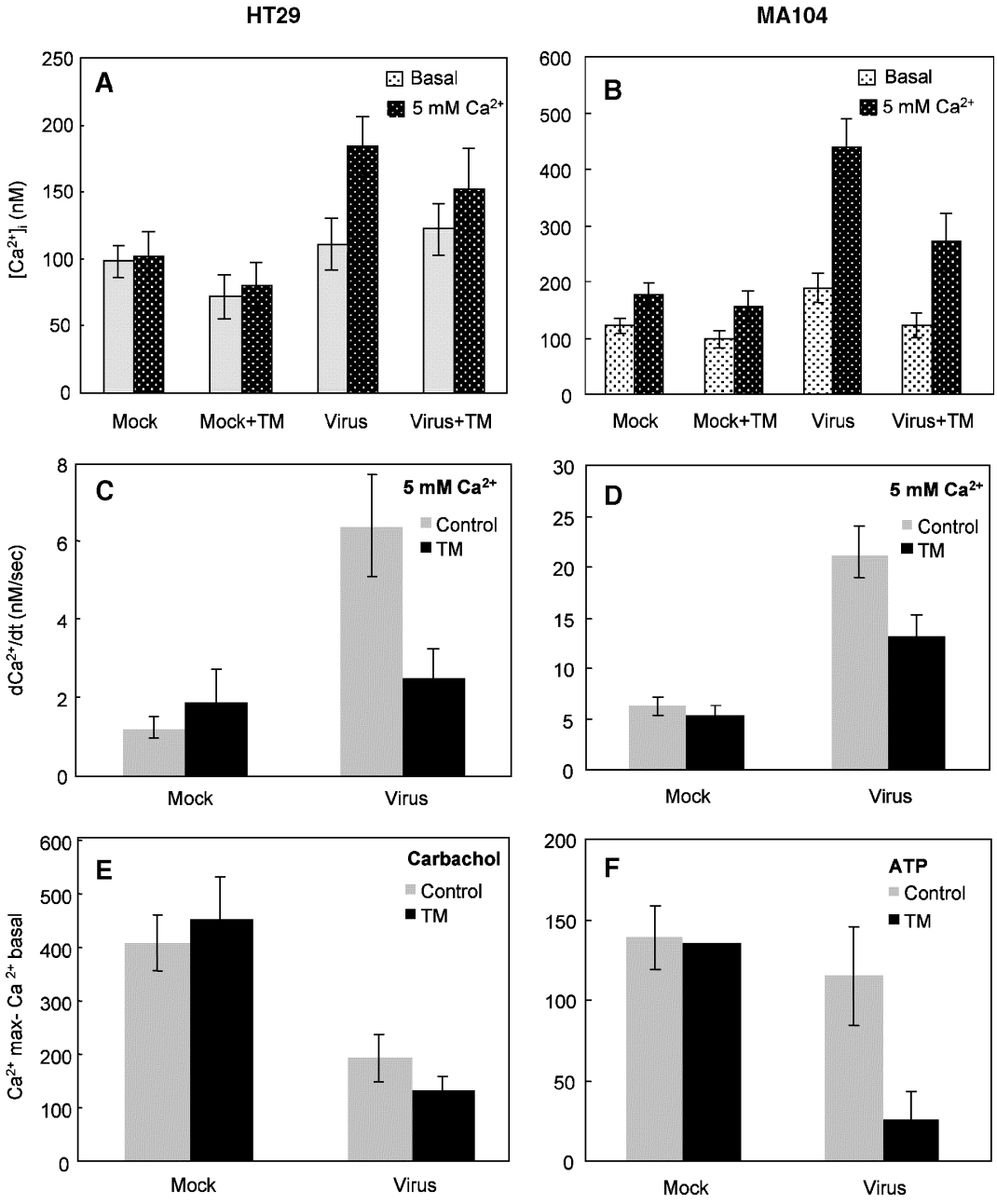

Fig. 3. Analysis of the effect of tunicamycin on plasma membrane permeability to Ca^{2+} and on agonist-releasable Ca^{2+} pools in rotavirus- or mock-infected HT29 and MA104 cells. In this figure we present a quantitative study of the experiments performed as in Fig. 2. In A and B, plotted data correspond to the mean ± standard error of the mean (SEM) of basal and maximal Ca^{2+} concentration before and after the addition of 5 mM Ca^{2+} to the extracellular medium in rotavirus-infected or non-infected HT29 (A) or MA 104 (B) cells in the presence or absence of tunicamycin. In C and D, plotted data correspond to the mean ± standard error of the mean (SEM) of initial rate of $[Ca^{2+}]_i$ change induced by the addition of 5 mM $CaCl_2$ to the extracellular medium (in A, B, C, and D, protocol corresponding to upper panels of Fig. 2; 6 sets of independent experiments for HT29 cells; 11 sets for MA104 cells). In E and F the experiments were performed as described in lower panels of Fig. 2. Data presented correspond to the mean ± SEM of the variation of cytosolic Ca^{2+} concentration induced by the addition of 10 μM carbachol (E) or 250 μM ATP (F) in rotavirus-infected or non-infected HT29 (E) and MA104 cells (F). The value corresponds to the mean of $[Ca]_{max} - [Ca]_{basal}$, where $[Ca]_{basal}$ and $[Ca]_{max}$ are the basal and maximal levels attained before or after the addition of the agonist in the different conditions (five sets of independent experiments in E and 4 sets in F).

traces). The initial rate of change of $[Ca^{2+}]_i$, dCa/dt, as well as the maximal $[Ca^{2+}]_i$ attained after the Ca^{2+} pulse was reduced in rotavirus-infected cells. This effect was better observed in MA104 cells (Figs. 7A–D). Brefeldin A did not modify the rate of entry in non-infected cells (Fig. 6, upper traces; Figs. 7C and D).

As shown in Figs. 1 and 2 virus infection decreased the amount of Ca^{2+} mobilized by agonists. However, in infected cells brefeldin A did not affect the state of filling of agonist sensitive sequestered Ca^{2+} pools beyond the effect of infection itself (Fig. 6, lower traces). The change in $[Ca^{2+}]_i$ induced by the release of stored Ca^{2+} elicited by carbachol or

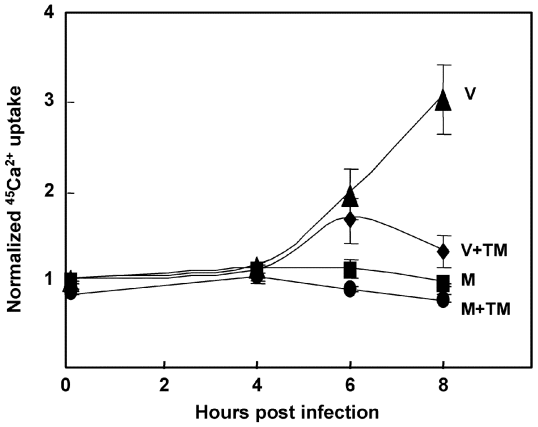

Fig. 4. Time course of the effect of tunicamycin on $^{45}Ca^{2+}$ uptake. Intracellular Ca^{2+} pools were evaluated by $^{45}Ca^{2+}$ uptake in mock (M) and rotavirus-infected (V) cells in the presence or absence of tunicamycin (Tm). Confluent monolayers of MA104 cells in 24-well plates were rotavirus infected (see Materials and methods). Tunicamycin (5 μg/ml) was added at 1 h post-infection, and $^{45}Ca^{2+}$ uptake measurements were performed at different hours post-infection. The time of uptake was 10 min. The counts obtained in virus-infected cells were normalized to mock-infected cells. The values correspond to the mean ± SEM of 20 measurements (five experiments and four replicates in each condition). Values at 8 h post-infection on virus-infected cells treated with tunicamycin were statistically different from virus-infected cells without drug ($P < 0.001$, paired t test).

ATP was similar in magnitude to that observed in untreated virus or mock-infected cells, respectively (Figs. 6 and 7E and F). Therefore, brefeldin A inhibits Ca^{2+} permeability of virus-infected cells without affecting agonist-releasable Ca^{2+} pools.

The addition of 5 mM Ca^{2+} after stimulation with carbachol or ATP leads to an increase in Ca^{2+} concentration in all conditions due to different components. The increase in Ca^{2+} concentration in brefeldin A treated or untreated mock-infected cells was small and probably due to capacitative Ca^{2+} entry. Again, the increase in virus-infected cells was large and reflected Ca^{2+} entry due to the activation of a virus-induced pathway and a capacitative component. In virus-infected cells treated with brefeldin A the permeability was rather small and similar to the mock-infected cells. This may suggest that brefeldin A inhibits the viral-activated component. The remnant permeability is perhaps due to capacitative entry linked to the depletion of stored Ca^{2+} pools.

We have also evaluated the effect of brefeldin A on total Ca^{2+} pools during the viral cycle, by measuring $^{45}Ca^{2+}$ uptake at 8 h post-infection (Fig. 8). Rotavirus infection of MA104 cells induced, in this series of experiments, an increase of Ca^{2+} uptake more than threefold with respect to the normalized value for mock-infected cells. The incubation in the presence of brefeldin A (8 μM) added from 1 h post-infection inhibited the increase in $^{45}Ca^{2+}$ uptake induced by infection, whereas brefeldin A had no effect in mock-infected cells. We also studied the effect of ATP as a Ca^{2+} mobilizing agonist from the ER on $^{45}Ca^{2+}$ uptake. Incubation with ATP (250 μM), during the last 30 min period before measurements at 8 h post-infection, did not induce a significant reduction of $^{45}Ca^{2+}$ uptake in rotavirus- or mock-infected cells.

Discussion

Calcium plays a critical role in the control of numerous cellular processes, both in physiological conditions and pathological states. The regulation of cytosolic Ca^{2+} concentration is a complex concert of events requiring the intervention of multiple pathways and mechanisms controlling influx and efflux. Calcium influx into the cytoplasm is the result of either Ca^{2+} release from intracellular stores (ER) via IP3 or ryanodine-sensitive channels, or Ca^{2+} influx across the plasma membrane through a variety of Ca^{2+}-permeable channels. Calcium efflux from the cytoplasm is the result of Ca^{2+} uptake by Ca^{2+} pumps of the ER (SERCA pump) and other transport mechanisms in other organelles, and extrusion by the Ca^{2+}-ATPase and other transporters like Na^{+}/Ca^{2+} exchange located at the plasma membrane (Carafoli, 2002).

Rotavirus infection of cultured cells affects several of these mechanisms. The end result is a progressive rise in cytosolic Ca^{2+} concentration. This arises as a primary event from an uncompensated increase in Ca^{2+} permeability of the plasma membrane (Michelangeli et al., 1991; Perez et al., 1999; Ruiz et al., 2000). The rise of $[Ca^{2+}]_i$ leads to an enhancement of sequestered $^{45}Ca^{2+}$, which is sensitive to thapsigargin (Michelangeli et al., 1995; Thastrup et al., 1990). The increase of Ca^{2+} permeability of the plasma membrane seems to be associated to the synthesis of a viral product.

This paper extends previous findings and provides insight into the mechanisms by which rotavirus infection increases Ca^{2+} permeability. In initial experiments (Fig. 1) we found

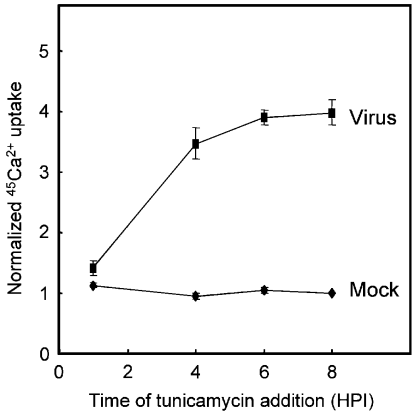

Fig. 5. Effect of tunicamycin added at different hours post-infection on $^{45}Ca^{2+}$ uptake in rotavirus- or mock-infected MA104 cells. The experiments were performed as in Fig. 4. In this series of experiments, tunicamycin (5 μg/ml) was added at 1, 4, or 6 hours post-infection, and $^{45}Ca^{2+}$ uptake was measured at 8 h post-infection. Values correspond to the mean ± SEM of eight measurements (two experiments and four replicates in each condition).

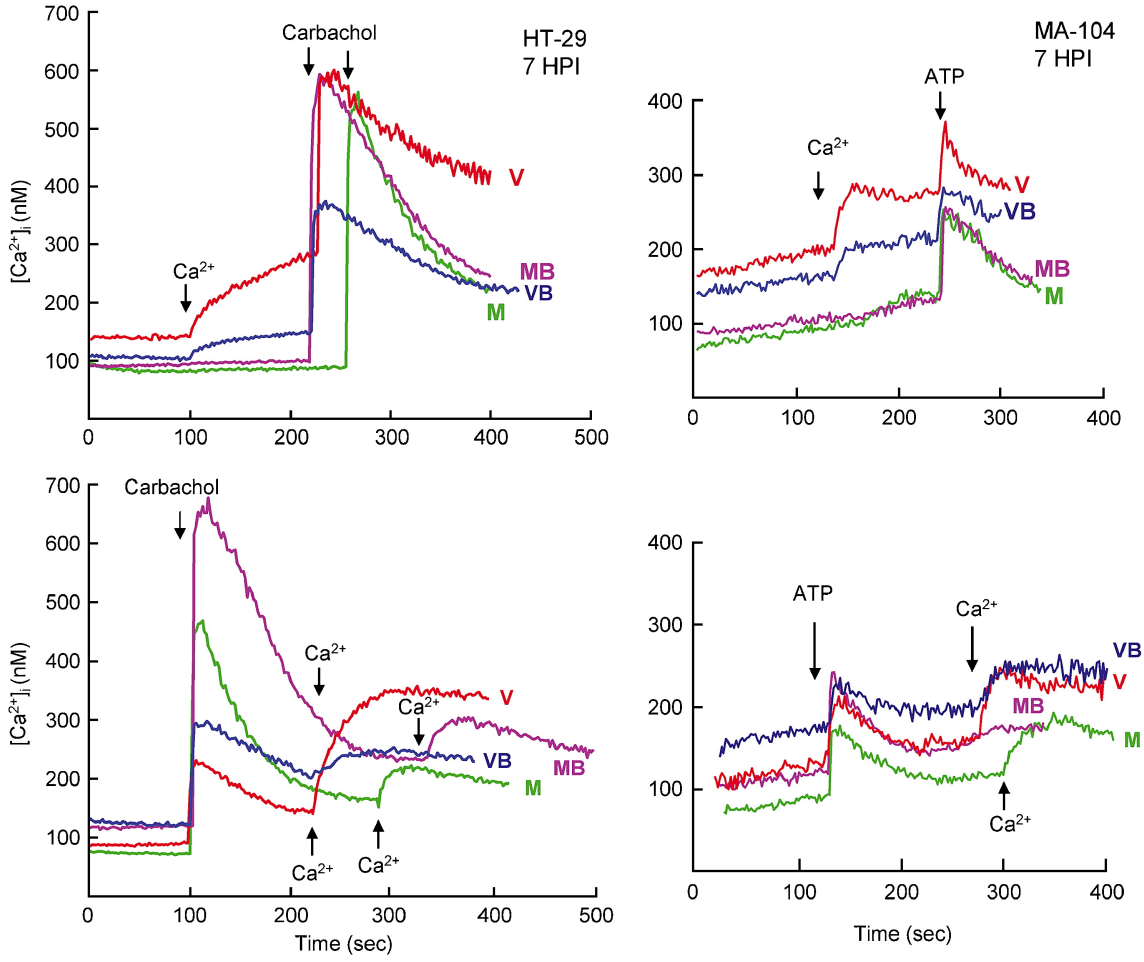

Fig. 6. Effect of brefeldin A on plasma membrane permeability to Ca^{2+} and on agonist-releasable Ca^{2+} pools in rotavirus- or mock-infected HT29 and MA104 cells. Confluent monolayers of HT29 and MA104 cells grown in 75 cm^2 falcon flasks were infected (see Materials and methods). Mock-infected cells were kept as controls. At 1 h post-infection the inoculum was removed and replaced by a medium with or without brefeldin A (8 μg/ml). At 7 h post-infection, measurement of $[Ca^{2+}]_i$ was performed by fura 2 fluorescence. Permeability to Ca^{2+} and the state of filling of agonist sensitive sequestered Ca^{2+} pools were evaluated as in Fig. 2. Traces of a representative experiment of a series are shown (rotavirus (V)- or mock (M)-infected cells; HT29 upper traces, $n = 5$; HT29 lower traces, $n = 8$; MA104 upper traces, $n = 10$; MA104 lower traces, $n = 5$).

that, in addition to increasing plasma membrane Ca^{2+} permeability and Ca^{2+} concentration, infection leads to a progressive depletion of agonist-releasable ER pools sensitive to thapsigargin, as measured by fura 2 fluorescence. On the other hand, the Ca^{2+} content measured by $^{45}Ca^{2+}$ uptake was enhanced along infection and was also sensitive to thapsigargin. In this case, infected MA104 cells showed a several fold increase in $^{45}Ca^{2+}$ uptake with respect to mock-infected ones (Michelangeli et al., 1991, 1995), whereas in HT29 cells it was small, attaining 1.5-fold (results not shown).

These results taken together appear contradictory. However, the two approaches may be measuring different ER pools both sensitive to thapsigargin. Agonists acting through IP3 liberate readily accessible free Ca^{2+} from the ER whereas $^{45}Ca^{2+}$ uptake estimates Ca^{2+} content both free and buffered inside the ER and other organelles. The sensitivity of $^{45}Ca^{2+}$ uptake to thapsigargin indicates that ER contributes to a major fraction of intracellular Ca^{2+}. In the ER these two pools, free and buffered, would be in equilibrium. Thapsigargin induces the emptying of all Ca^{2+} stores dependent on the activity of the SERCA pump. On the other hand, the IP3-dependent agonists may release only a fraction of these stores. The ability of these agonists to release Ca^{2+} may be related to different mechanisms, among others, compartmentalization of the ER, heterogeneity of IP3 receptors in the ER membrane, or down-regulation or inactivation of agonist receptors at the plasma membrane level. Furthermore, rotavirus infection could alter the expression of receptors on the cell surface as described for other viruses (Gonzalez and Carrasco, 2003; Neznanov et al., 2001).

Our results suggest that rotavirus infection decreases free Ca^{2+} whereas increases Ca^{2+} bound to buffers inside the ER. Such buffers may be directly linked to the viral cycle. In this sense, VP7, which is accumulated during infection inside the ER, is known to bind Ca^{2+} (Dormitzer and Greenberg, 1992; Dormitzer et al., 2000). Other Ca^{2+} binding cellular proteins

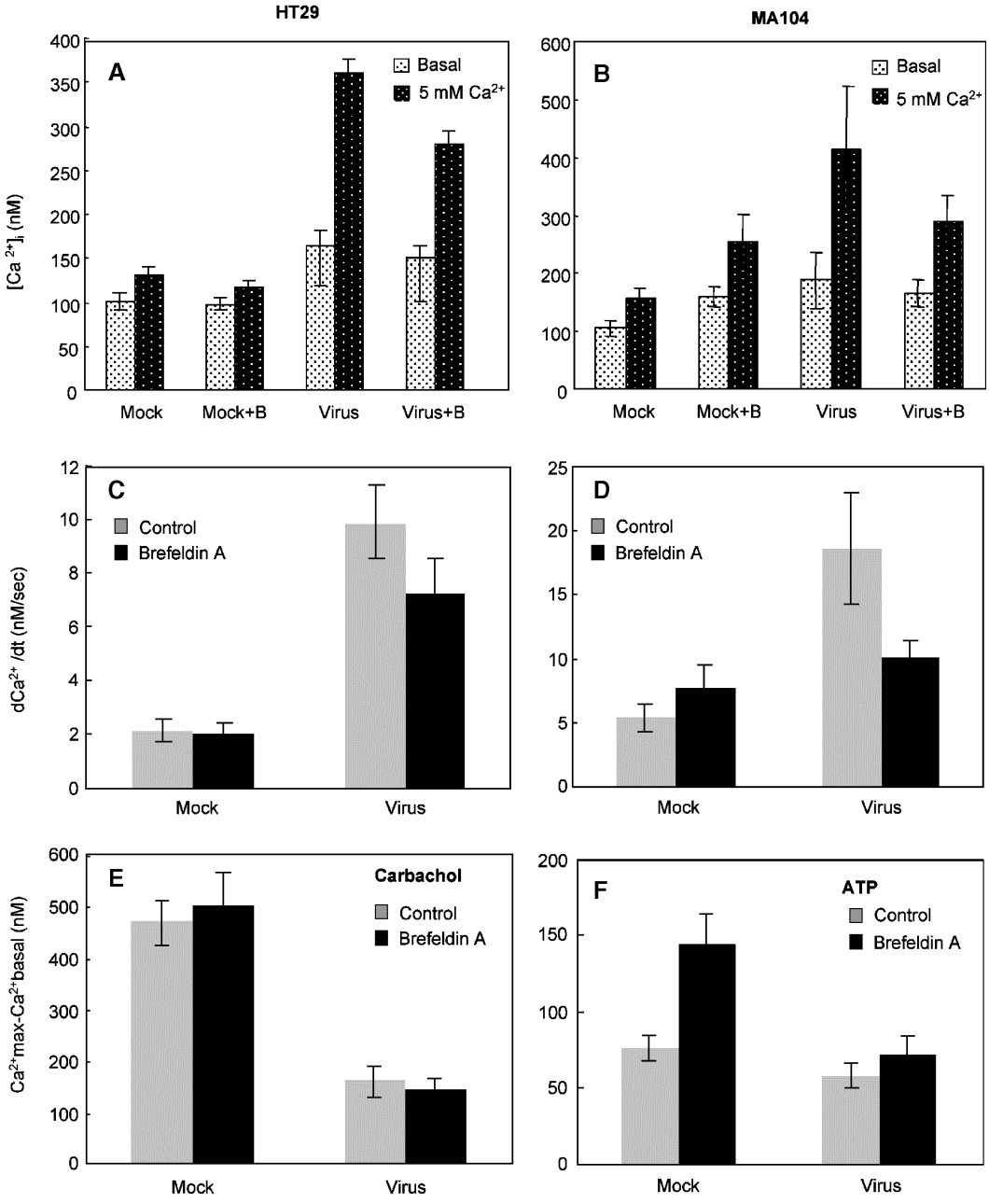

Fig. 7. Analysis of the effect of brefeldin A on plasma membrane permeability to Ca^{2+} and on agonist-releasable Ca^{2+} pools in rotavirus- or mock-infected HT29 and MA104 cells. Quantitative study of experiments performed as in Fig. 6. In A and B, plotted data correspond to the mean ± standard error of the mean (SEM) of basal and maximal Ca^{2+} concentration before and after the addition of 5 mM Ca^{2+} to the extracellular medium in rotavirus-infected or non-infected HT29 (A) or MA 104 (B) cells in the presence or absence of brefeldin A. In C and D, plotted data correspond to the mean ± standard error of the mean (SEM) of initial rate of $[Ca^{2+}]_i$ change induced by the addition of 5 mM $CaCl_2$ to the extracellular medium (in A, B, C, and D, protocol corresponding to upper panels of Fig. 6; 5 sets of independent experiments in HT29 cells and 10 sets in MA104 cells). In E and F, the experiments were performed as described in lower panels of Fig. 6. Data presented correspond to the mean ± SEM of the variation of cytosolic Ca^{2+} concentration induced by the addition of 10 μM carbachol (E) or 250 μM ATP (F) in rotavirus- or non-infected HT29 (E) and MA104 cells (F). The value is the mean of $[Ca]_{max} - [Ca]_{basal}$, where $[Ca]_{basal}$ and $[Ca]_{max}$ are the basal and maximal levels attained before or after the addition of the agonist in the different conditions (eight sets of independent experiments in B and 5 sets in D).

and chaperones may be over expressed in infected cells and may play a role in the total Ca^{2+} buffering capacity (Xu et al., 1998).

The decrease of agonist-releasable ER Ca^{2+} pools raises the question as to whether virus infection increases plasma membrane Ca^{2+} permeability by activating a capacitative pathway. Our results show that in the two cell types the emptying of the ER Ca^{2+} pools by agonists activates a capacitative channel in mock-infected cells. However, the increase in Ca^{2+} permeability observed in virus-infected cells was much higher than what can be accounted for by the capacitative component. These results strongly support the

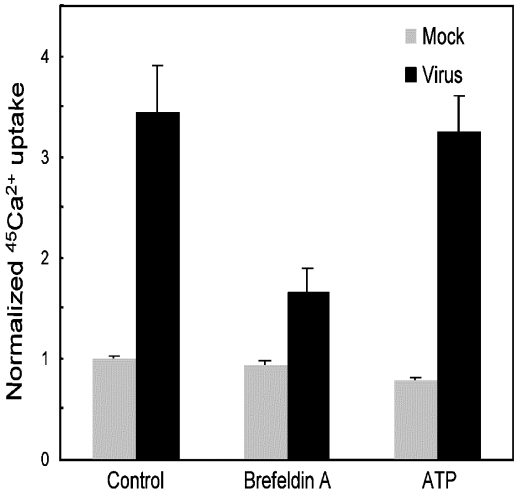

Fig. 8. Effect of brefeldin A and ATP on $^{45}Ca^{2+}$ uptake in rotavirus- or mock-infected MA104 cells. Confluent monolayers of MA104 cells grown in 24-well plates were infected (see Materials and methods). Mock-infected cells were kept as controls. Intracellular Ca^{2+} pools were evaluated at 8 h post-infection by $^{45}Ca^{2+}$ uptake in mock (M) and rotavirus-infected (V) cells in the presence or absence of brefeldin A from 1 h post-infection or after treatment with ATP (250 μM) during the last 30 min of the infection period. The time of $^{45}Ca^{2+}$ uptake was 10 min. The counts obtained in virus-infected cells were normalized to mock-infected cells. The values correspond to the mean ± SEM of 12 measurements (four experiments and three replicates in each condition).

hypothesis of the involvement of a Ca^{2+} pathway directly induced by virus infection.

Tunicamycin is an inhibitor of N-glycosylation of ER proteins. In rotavirus infection it blocks VP7 and NSP4 glycosylation and the production of infectious viral particles, provoking the accumulation of intermediate enveloped non-infectious virions in the ER (Petrie et al., 1983; Sabara et al., 1982). Tunicamycin reduced the increase in plasma membrane Ca^{2+} permeability induced by rotavirus infection and the size of the pools releasable by agonists measured by fura 2, as well as those measured by $^{45}Ca^{2+}$ uptake. The use of tunicamycin to prevent glycosylation of viral proteins permitted to assess the involvement of NSP4 and/or VP7 in these effects. The inhibition by tunicamycin of the increase in plasma membrane Ca^{2+} permeability induced by rotavirus infection may suggest that a glycosylated viral protein forms a viral channel or activates a cellular one. In the first case, the viral protein would traffic from the ER to the plasma membrane. In this sense, a truncated form of a recombinant NSP4 expressed in Vero cells corresponding to the transmembrane segment (1– 89 aa) of the molecule was able to escape the ER via a brefeldin A-sensitive pathway and reach the plasma membrane (Mirazimi et al., 2003). One might speculate that during rotavirus infection some glycosylated NSP4 molecules could travel to the plasma membrane after protease cleavage of the cytoplasmic tail whereas this last one would be secreted to the extracellular medium by a yet unknown mechanism (Zhang et al., 2000). On the other hand, the full-length NSP4 molecule has been recently detected at the plasma membrane in rotavirus-infected cells (Mitchell and Ball, 2004; Storey and Ball, 2004). Alternatively, glycosylation of NSP4 may be involved in the putative targeting of the full-length NSP4 or an N-terminal peptide to the plasma membrane. In infected cells treated with tunicamycin, the unglycosylated NSP4 might be retained in the ER membrane and unable to travel to the plasma membrane. The accumulation of this unglycosylated product in the ER might be responsible for the emptying of Ca^{2+} pools observed in infected cells treated with tunicamycin. Perhaps the accumulation of unglycosylated NSP4 occurs normally along infection and might be responsible for the depletion of the ER pools at the end of the viral cycle. In this sense, an increase of ER permeability has been described late during infection in Caco2 cells (Brunet et al., 2000) and sf9 cells expressing NSP4 (Tian et al., 1995).

The inhibitory effect of brefeldin A on the increase of permeability elicited by infection found in this paper supports the hypothesis that protein trafficking of a viral product is required to increase plasma membrane permeability. Brefeldin A is a fungal macrocyclic lactone which inhibits protein trafficking in the endomembrane system of mammalian cells, disassembles Golgi membranes, and provokes the loss of Cop I coats from the Golgi apparatus (Lippincott-Schwartz et al., 1991). On the other hand, brefeldin A promotes retrograde transport of Golgi components to the ER. Brefeldin A did not seem to change rotavirus antigenicity but affected the electrophoretic mobility on the ER resident VP7 and NSP4 proteins without effect on cytosolic capsid proteins. As in the case of tunicamycin, brefeldin A inhibited the production of infectious viral particles and induced the accumulation of intermediate enveloped virions in the ER (Mirazimi et al., 1996).

We have also shown here that brefeldin A prevents the increase of $^{45}Ca^{2+}$ pools induced by infection. This may mean that there is a leak in the ER membrane. The retention of a putative Ca^{2+} channel in this compartment could be responsible for this effect. Alternatively, the alteration of processing of VP7 may change its conformation affecting the putative Ca^{2+} buffering capacity and therefore decreasing the size of the $^{45}Ca^{2+}$ pools.

In conclusion, our results support the hypothesis that a glycosylated viral product travels to the plasma membrane to form a Ca^{2+} channel and hence elevate Ca^{2+} permeability. We have interpreted our findings in the light of the effects of NSP4 on Ca^{2+} homeostasis. However, we cannot exclude the intervention of the other glycosylated rotavirus protein VP7 and even cellular proteins, given the fact that different viral products can interact at the membrane level to modify ionic permeability. It is known that VP5 and peptides of VP7 are also able to destabilize membranes and increase permeability (Charpilienne et al., 1997; Denisova et al., 1999). On the other hand VP7 has not been detected at plasma membrane surface but associated to VP4 which was biotinylated at the surface of the infected cell (Nejmeddine et al., 2000).

The effects of rotavirus infection on plasma membrane Ca^{2+} permeability do not appear to be mediated by the de

novo synthesis of a cellular protein since these effects were not blocked by actinomycin D. Further support for this contention comes from the finding that enhancement of the sequestered $^{45}Ca^{2+}$ pools was not blocked either by this agent (Michelangeli et al., 1991). Moreover, it is known that the synthesis of cellular proteins is inhibited in the early stages of rotavirus infection (Estes and Cohen, 1989; Piron et al., 1998). However, we cannot at this point completely discard the intervention of an already present cellular protein activated by infection. The translation of long-lived cellular mRNAs could be stimulated as the result of rotavirus infection. If this were the case, the cellular protein would be synthesized as an integral ER glycoprotein and traffic to the plasma membrane by a brefeldin A-sensitive pathway. Alternatively, the newly synthesized cellular protein could act as a messenger to stimulate the opening of viral or preexisting cellular Ca^{2+} channels. It is clear that lacking so far identification of the putative channel, a number of explanations for the results are possible. However, the simplest unifying hypothesis is that these effects are mediated by the synthesis of a viral glycoprotein.

Within our hypothesis, NSP4 would be acting as a viroporin. These are a group of small proteins (~100 aa) that participate at different stages of the viral cycle and affect cellular functions, including the cell vesicle system, glycoprotein trafficking, and membrane permeability (Gonzalez and Carrasco, 2003; Neznanov et al., 2001). Viroporins have a hydrophobic transmembrane domain that interacts with the lipid bilayer. Viroporin oligomerization may give rise to hydrophilic pores at the membranes of virus-infected cells enhancing the passage of ions and small molecules (Fischer and Sansom, 2002; Gonzalez and Carrasco, 2003). Viruses representative of around 10 viral families have been shown to express such proteins. Among these, recent research efforts focus on the actions of the viral proteins influenza virus M2, poliovirus 2B, alphavirus 6K, HIV-1 Vpu, and HCV p7, which has been shown to function as a Ca^{2+} channel (Gonzalez and Carrasco, 2003; Nieva et al., 2003; Premkumar et al., 2004; Vijayvergiya et al., 2004).

Materials and methods

Cell cultures and virus infection

MA104 cells (embryonic rhesus monkey kidney cells, kindly supplied by J. Cohen) and the colon carcinoma cells HT29 (from ATCC) were used. MA104 cells were grown in Minimum Essential Medium (MEM GIBCO cat 61100) and HT29 cells in Dulbecco's modified Eagle Medium (DMEM containing 4500 mg/l glucose form GIBCO, cat 12100) and maintained as previously described (Michelangeli et al., 1995).

The OSU strain of rotavirus (porcine, serotype P9[7]G5 [5], kindly supplied by F. Liprandi, Instituto Venezolano de Investigaciones Científicas, Caracas, Venezuela) was used in all experiments. Rotaviruses were replicated in MA104 cells in the presence of trypsin (1 μg/ml). Infection was carried out for 1 h at 37 °C. Then, the inoculum was removed, washed with PBS, and further incubated with MEM without fetal calf serum until complete cytopathic effect. Cell suspensions were frozen–thawed twice, clarified by centrifugation. Viral suspensions were treated with 10 μg of trypsin per ml for 30 min at 37 °C to cleave VP4 (Trypsin Type IX; Sigma). Infectivity titers of the preparations used were measured by titration in microplates in MA104 cells and HT29 cells using anti-VP6 monoclonal antibody (4B2D2) for indirect immunofluorescence staining after methanol fixation and expressed as fluorescent-focus units (FFU) (Ciarlet et al., 1995).

Determination of intracellular Ca^{2+} concentration

MA104 and HT29 cells were seeded in 75 cm^2 falcon flasks at a density of 3 × 105 cells/flask in minimal essential medium (MEM) supplemented with 10% fetal calf serum and used at confluency 5–7 days later. Monolayers were infected by OSU rotavirus at a multiplicity of infection of approximately of 20 FFU/cell. At the end of the infection period, cells were detached from the flask by trypsin treatment, washed by centrifugation, and resuspended in a medium containing (in mM): NaCl, 130; KCl, 5; CaCl2, 1; MgCl2, 1; HEPES, 20 (pH 7.2); and 0.1% albumin (w/v) at an approximate concentration of 8 × 10^6 cells/ml. Cell suspensions were incubated with 10 μM fura 2 AM with pluronic (2%) for 30 min, washed twice by centrifugation, resuspended in buffer, and maintained at room temperature. For measurements, aliquots of the cell suspension were newly washed and resuspended in 1.2 ml of the same medium without albumin. Fluorescence was measured at 37 °C in a spectrofluorometer (Photon Technology International) equipped with stirrer and temperature control. Excitation wavelengths were 340 and 380 nm, which were alternatively changed by computer control allowing acquisition of one pair of data per second. Emission was fixed at 510 nm. The ratio of the fluorescent signal measured at 340 and 380 nm was computer determined. Intracellular free Ca^{2+} concentration, $[Ca^{2+}]_i$, was calculated according to the equation described by Grynkiewicz et al. (1985), using an apparent kDa for fura 2-Ca of 224 nM. Maximal fluorescence ratio (R_{max}) was determined by addition of digitonin (80 μg/ml) to permeabilize cells and minimal fluorescence ratio (R_{min}) by the subsequent addition of 80 mM EGTA in Tris (0.1 M) pH 7.4 buffer.

$^{45}Ca^{2+}$ uptake

Cell monolayers were grown to confluency in 24-well Linbro plates for 3–4 days. At this stage, cells were not differentiated (Ciarlet et al., 2001). Cell infection was performed at a multiplicity of infection of approximately 20 FFU/cell. In these conditions all cells in the monolayer

were infected during the first cycle as ascertained by immunofluorescence of VP6. At the end of the infection period maintenance medium was removed and replaced by 200 μl of MEM containing 45 Ca^{2+} (1 μCi per well). Uptake was stopped after 10 min by washing the cells four times by immersion in ice-cold PBS. After air drying, cells were dissolved in 250 μl of 0.1% SDS. Radioactivity was determined in aliquots by liquid scintillation counting. As the number of cells per well was found to be constant, uptake values for single experiments are normalized and expressed as the relation to counts in mock-infected wells.

Acknowledgments

The authors wish to thank Dr. J.F. Perez for his participation in preliminary experiments and Y. Higuerey for technical assistance. This work was supported in part by FONACIT (Venezuela) grant 2001000329.

References

Berkova, Z., Morris, A.P., Estes, M.K., 2003. Cytoplasmic calcium measurement in rotavirus enterotoxin-enhanced green fluorescent protein (NSP4-EGFP) expressing cells loaded with Fura-2. Cell Calcium 34 (1), 55–68.

Brunet, J.P., Cotte-Laffitte, J., Linxe, C., Quero, A.M., Geniteau-Legendre, M., Servin, A., 2000. Rotavirus infection induces an increase in intracellular calcium concentration in human intestinal epithelial cells: role in microvillar actin alteration. J. Virol. 74 (5), 2323–2332.

Carafoli, E., 2002. Calcium signaling: a tale for all seasons. Proc. Natl. Acad. Sci. U.S.A. 99 (3), 1115–1122.

Carrasco, L., 1995. Modification of membrane permeability by animal viruses. Adv. Virus Res. 45, 61–112.

Charpilienne, A., Abad, M.J., Michelangeli, F., Alvarado, F., Vasseur, M., Cohen, J., Ruiz, M.C., 1997. Solubilized and cleaved VP7, the outer glycoprotein of rotavirus, induces permeabilization of cell membrane vesicles. J. Gen. Virol. 78 (Pt. 6), 1367–1371.

Ciarlet, M., Ludert, J.E., Liprandi, F., 1995. Comparative amino acid sequence analysis of the major outer capsid protein (VP7) of porcine rotaviruses with G3 and G5 serotype specificities isolated in Venezuela and Argentina. Arch. Virol. 140 (3), 437–451.

Ciarlet, M., Crawford, S.E., Estes, M.K., 2001. Differential infection of polarized epithelial cell lines by sialic acid-dependent and sialic acid-independent rotavirus strains. J. Virol. 75 (23), 11834–11850.

del Castillo, J.R., Ludert, J.E., Sanchez, A., Ruiz, M.C., Michelangeli, F., Liprandi, F., 1991. Rotavirus infection alters Na+ and K+ homeostasis in MA-104 cells. J. Gen. Virol. 72, 541–547.

Delmas, O., Gardet, A., Chwetzoff, S., Breton, M., Cohen, J., Colard, O., Sapin, C., Trugnan, G., 2004. Different ways to reach the top of a cell. Analysis of rotavirus assembly and targeting in human intestinal cells reveals an original raft-dependent, Golgi-independent apical targeting pathway. Virology 327 (2), 157–161.

Denisova, E., Dowling, W., LaMonica, R., Shaw, R., Scarlata, S., Ruggeri, F., Mackow, E.R., 1999. Rotavirus capsid protein VP5* permeabilizes membranes. J. Virol. 73 (4), 3147–3153.

Dormitzer, P.R., Greenberg, H.B., 1992. Calcium chelation induces a conformational change in recombinant herpes simplex virus-1-expressed rotavirus VP7. Virology 189, 828–832.

Dormitzer, P.R., Greenberg, H.B., Harrison, S.C., 2000. Purified recombinant rotavirus VP7 forms soluble, calcium-dependent trimers. Virology 277 (2), 420–428.

Estes, M.K., 1996. Rotaviruses and their replication. In: Fields, B.N., Knipe, P.M., Howley, P.M., Chanock, R.M., Melnick, J.L., Monath, T.P., Roizman, B., Straus, S.E. (Eds.). Fields Virology, vol. 2 (3rd ed.). Lippincott-Raven Publishers, Philadelphia, pp. 1625–1655. 2 vols.

Estes, M.K., 2003. The rotavirus NSP4 enterotoxin: current status and challenges. In: Dusselberger, U., Gray, J. (Eds.). Viral Gastroenteritis, vol. 9. Elsevier, Amsterdam, pp. 207–224.

Estes, M.K., Cohen, J., 1989. Rotavirus gene structure and function. Microbiol. Rev. 53, 410–499.

Estes, M.K., Kang, G., Zeng, C.Q., Crawford, S.E., Ciarlet, M., 2001. Pathogenesis of rotavirus gastroenteritis. Novartis Found. Symp. 238, 82–96.

Fischer, W.B., Sansom, M.S., 2002. Viral ion channels: structure and function. Biochim. Biophys. Acta 1561 (1), 27–45.

Gonzalez, M.E., Carrasco, L., 2003. Viroporins. FEBS Lett. 552 (1), 28–34.

Grynkiewicz, G., Poenie, M., Tsien, R.Y., 1985. A new generation of Ca^{2+} indicators with greater improved fluorescence properties. J. Biol. Chem. 260, 3440–3450.

Jourdan, N., Maurice, M., Delautier, D., Quero, A.M., Servin, A.L., Trugnan, G., 1997. Rotavirus is released from the apical surface of cultured human intestinal cells through nonconventional vesicular transport that bypasses the Golgi apparatus. J. Virol. 71 (11), 8268–8278.

Lippincott-Schwartz, J., Yuan, L., Tipper, C., Amherdt, M., Orci, L., Klausner, R.D., 1991. Brefeldin A's effects on endosomes, lysosomes, and the TGN suggest a general mechanism for regulating organelle structure and membrane traffic. Cell 67 (3), 601–616.

Michelangeli, F., Ruiz, M.C., 2003. Physiology and pathophysiology of the gut in relation to viral diarrhea. In: Dusselberger, U., Gray, J. (Eds.). Viral Gastroenteritis, vol. 9. Elsevier, Amsterdam, pp. 23–50.

Michelangeli, F., Ruiz, M.C., del Castillo, J.R., Ludert, J.E., Liprandi, F., 1991. Effect of rotavirus infection on intracellular calcium homeostasis in cultured cells. Virology 181, 520–527.

Michelangeli, F., Liprandi, F., Chemello, M.E., Ciarlet, M., Ruiz, M.C., 1995. Selective depletion of stored calcium by thapsigargin blocks rotavirus maturation but not the cytopathic effect. J. Virol. 69 (6), 3838–3847.

Mirazimi, A., von Bonsdorff, C.H., Svensson, L., 1996. Effect of brefeldin A on rotavirus assembly and oligosaccharide processing. Virology 217, 554–563.

Mirazimi, A., Magnusson, K.E., Svensson, L., 2003. A cytoplasmic region of the NSP4 enterotoxin of rotavirus is involved in retention in the endoplasmic reticulum. J. Gen. Virol. 84 (Pt. 4), 875–883.

Mitchell, D.A., Ball, J.M., 2004. NSP4 is transported to both apical and basolateral surface of intestinal epithelial cells. American Society for Virology, 23rd Annual Meeting (Abstract), p. 184. Quebec, Canada.

Nejmeddine, M., Trugnan, G., Sapin, C., Kohli, E., Svensson, L., Lopez, S., Cohen, J., 2000. Rotavirus spike protein VP4 is present at the plasma membrane and is associated with microtubules in infected cells. J. Virol. 74 (7), 3313–3320.

Neznanov, N., Kondratova, A., Chumakov, K.M., Angres, B., Zhumabayeva, B., Agol, V.I., Gudkov, A.V., 2001. Poliovirus protein 3A inhibits tumor necrosis factor (TNF)-induced apoptosis by eliminating the TNF receptor from the cell surface. J. Virol. 75 (21), 10409–10420.

Nieva, J.L., Agirre, A., Nir, S., Carrasco, L., 2003. Mechanisms of membrane permeabilization by picornavirus 2B viroporin. FEBS Lett. 552 (1), 68–73.

Orci, L., Tagaya, M., Amherdt, M., Perrelet, A., Donaldson, J.G., Lippincott-Schwartz, J., Klausner, R.D., Rothman, J.E., 1991. Brefeldin A, a drug that blocks secretion, prevents the assembly of non-clathrin-coated buds on Golgi cisternae. Cell 64 (6), 1183–1195.

Perez, J.F., Ruiz, M.C., Chemello, M.E., Michelangeli, F., 1999. Characterization of a membrane calcium pathway induced by rotavirus infection in cultured cells. J. Virol. 73 (3), 2481–2490.

Petrie, B.L., Estes, M.K., Graham, D.Y., 1983. Effects of tunicamycin on rotavirus morphogenesis and infectivity. J. Virol. 46, 270–274.

Piron, M., Vende, P., Cohen, J., Poncet, D., 1998. Rotavirus RNA-binding protein NSP3 interacts with eIF4GI and evicts the poly(A) binding protein from eIF4F. EMBO J. 17 (19), 5811–5821.

Premkumar, A., Wilson, L., Ewart, G.D., Gage, P.W., 2004. Cation-selective ion channels formed by p7 of hepatitis C virus are blocked by hexamethylene amiloride. FEBS Lett. 557 (1–3), 99–103.

Ruiz, M.C., Cohen, J., Michelangeli, F., 2000. Role of Ca(2+) in the replication and pathogenesis of rotavirus and other viral infections. Cell Calcium 28 (3), 137–149.

Sabara, M., Balbiuk, L.A., Gilchrist, J., Misra, V., 1982. Effect of tunicamycin on rotavirus assembly and infectivity. J. Virol. 43, 1082–1090.

Storey, S.M., Ball, J.M., 2004. Identification of endogenously expressed rotavirus enterotoxin in plasma membrane-derived caveolae. American Society for Virology, 23rd Annual Meeting (Abstract), p. 274. Quebec, Canada.

Thastrup, O., Cullen, P.J., Drobak, B.K., Hanley, M.R., Dawson, A.P., 1990. Thapsigargin, a tumor promoter, discharges intracellular Ca^{2+} stores by specific inhibition of the endoplasmic reticulum Ca2(+)-ATPase. Proc. Natl. Acad. Sci. U. S. A. 87 (7), 2466–2470.

Tian, P., Hu, Y., Schilling, W.P., Lindsay, D.A., Eiden, J., Estes, M.K., 1994. The nonstructural glycoprotein of rotavirus affects intracellular calcium levels. J. Virol. 68, 251–257.

Tian, P., Estes, M.K., Hu, Y., Ball, J.M., Zeng, C.Q., Schilling, W.P., 1995. The rotavirus nonstructural glycoprotein NSP4 mobilizes Ca^{2+} from the endoplasmic reticulum. J. Virol. 69 (9), 5763–5772.

Vijayvergiya, V., Wilson, R., Chorak, A., Gao, P.F., Cross, T.A., Busath, D.D., 2004. Proton conductance of influenza virus m2 protein in planar lipid bilayers. Biophys. J. 87 (3), 1697–1704.

Xu, A., Bellamy, A.R., Taylor, J.A., 1998. BiP (GRP78) and endoplasmin (GRP94) are induced following rotavirus infection and bind transiently to an endoplasmic reticulum-localized virion component. J. Virol. 72 (12), 9865–9872.

Zhang, M., Zeng, C.Q., Morris, A.P., Estes, M.K., 2000. A functional NSP4 enterotoxin peptide secreted from rotavirus-infected cells [in process citation]. J Virol 74 (24), 11663–11670.